Published in final edited form as:
Biochim Biophys Acta. 2010 ; 1799(5-6): 480–486. doi:10.1016/j.bbagrm.2010.01.009.

Structural characterization of H3K56Q nucleosomes and nucleosomal arrays

Shinya Watanabe[1,*], **Michael Resch**[2,*], **Wayne Lilyestrom**[2], **Nicholas Clark**[2], **Jeffrey C. Hansen**[2], **Craig Peterson**[1], and **Karolin Luger**[2,3]

[1] Program in Molecular Medicine, University of Massachusetts Medical School, 373 Plantation St.; Worcester, Massachusetts 01605

[2] Department of Biochemistry and Molecular Biology, Colorado State University, Fort Collins, CO 80523-1870

[3] Howard Hughes Medical Institute

Abstract

The posttranslational modification of histones is a key mechanism for the modulation of DNA accessibility. Acetylated lysine 56 in histone H3 is associated with nucleosome assembly during replication and DNA repair, and is thus likely to predominate in regions of chromatin containing nucleosome free regions. Here we show by x-ray crystallography that mutation of H3 lysine 56 to glutamine (to mimic acetylation) or glutamate (to cause a charge reversal) has no detectable effects on the structure of the nucleosome. At the level of higher order chromatin structure, the K to Q substitution has no effect on the folding of model nucleosomal arrays in cis, regardless of the degree of nucleosome density. In contrast, defects in array-array interactions in trans ('oligomerization') are selectively observed for mutant H3 lysine 56 arrays that contain nucleosome free regions. Our data suggests that H3K56 acetylation is one of the molecular mechanisms employed to keep chromatin with nucleosome free regions accessible to the DNA replication and repair machinery.

Introduction

Nucleosomes, the basic building blocks of chromatin, are formed by coiling 147 base pairs of DNA around a protein core that consists of two copies each of histones H2A, H2B, H3 and H4 [1]. Hundreds of thousands of nucleosomes arrayed on chromosomal DNA undergo hierarchical condensation steps to achieve the degree of compaction that is necessary to fit the entire eukaryotic genome into the confines of the nucleus [2]. Properties that regulate the degree of compaction of nucleosomes and chromatin (e.g., histone saturation levels, histone variants, and post-translational modifications) will either locally or globally affect DNA accessibility to permit access to the genome.

Posttranslational modifications of histones have emerged as a key mechanism to regulate important biological processes such as transcription, DNA repair, and replication (reviewed for example in [3,4]). Numerous side chains in the histone tails, and an increasing number of

Correspondence to: Jeffrey C. Hansen; Craig Peterson; Karolin Luger.

*These authors contributed equally to this work

amino acids in the structured regions of the histones, are the targets of tightly regulated and highly specific activities that add or remove chemical modifications to specific locations in chromatin in response to biological cues (reviewed in [3,5,6]). Modern techniques identify new post-translational modifications at a rapid rate; however, our understanding of the mechanisms by which the chemical modification of selected histone residues affects chromatin biology has lagged behind. In many cases, specifically modified histone tails in turn recruit specific activities required for the required task (e.g. DNA repair, transcription, etc.; [7]). Recent structural work has confirmed the notion that the structure of the nucleosome itself is not greatly affected by histone modifications [8]. However, modification of certain residues has pronounced effects on the ability of nucleosomal array to fold and compact into higher order structures of increasing complexity [8–10].

Recently, the acetylation of H3K56 has received much attention due to its implied biological roles in transcription, DNA repair, and in maintaining genomic stability [11–14]. The modification is added onto non-nucleosomal H3 by the HAT Rtt109 (in yeast) or p300 (in metazoans) and is subsequently incorporated into nucleosomes. H3K56ac is a marker for newly synthesized histones during replication ([15] and references therein), and is also implicated in creating a favorable chromatin environment for DNA repair [16,17]. Additionally, it plays a role in chromatin disassembly during transcriptional activation [11,12]. Because of the location of this residue in the structured region of H3 near the DNA at its entry- and exit point [1] it has been speculated that acetylation may destabilize the nucleosome sufficiently to account for some of the observed biological effects [18].

A recent exciting technical development now allows genetic encoding of N(epsilon)-acetyllysine into recombinant proteins in specific positions [19]. This has enabled a first analysis of nucleosomes and nucleosomal arrays reconstituted with histone H3 specifically acetylated at K56 [20]. These studies showed that H3K56ac does not affect salt-dependent nucleosome stability, but that moderately increased ‘breathing’ of the DNA ends can be observed in H3K56ac nucleosomes. It was further shown that there is no effect of this modification on the salt-dependent compaction of saturated nucleosomal arrays with and without linker histone H5. However, a long saturated array of nucleosomes with linker histone does not mimic the natural chromatin configurations in which H3K56ac is found (see above). Due to the preponderance of H3K56ac in regions of active transcription and near sites of replication- and repair-coupled DNA assembly, this modification should also be studied in the context of subsaturated chromatin depleted of nucleosomes and linker histone, i.e., nucleosomal arrays containing nucleosome-free regions.

Here we present two crystal structures of nucleosomes in which H3K56 has been substituted with either glutamine to mimic acetylation, or with glutamic acid to introduce a charge reversal at this location. Our data indicate that the structure of the nucleosome remains unaffected by these changes. We also analyze the folding and oligomerization properties of subsaturated and saturated nucleosomal arrays bearing K56Q and find that this substitution negatively affects the ability of the arrays to oligomerize when they are subsaturated and contain nucleosome-free “gaps” in the arrays. No effects of K56Q were observed at the level of local array folding. Our data suggests that the acetylation of H3K56 results in a more globally open and accessible chromatin structure in regions of the genome depleted of nucleosomes.

Materials and Methods

Proteins and DNA

Histone expression and purification was performed as described previously [21]. The 147 bp palindromic α-sat DNA was purified as described [21]. The 208-12 5S rDNA repeat used to prepare model nucleosomal arrays was purified following published procedures [22,23].

Reconstitution of nucleosomes and nucleosomal arrays

Nucleosomes were reconstituted onto palindromic 146 bp DNA fragment derived from α-satellite DNA as previously described [1,21]. Briefly, equal molar ratios of histone octamers containing H3K56Q or H3K56E were mixed with 147 bp α-sat DNA in TE buffer (10mM Tris-HCl, 0.25 mM EDTA, pH 7.5) containing 2.0 M KCl_2. and dialyzed using salt gradient dialysis into TE buffer (0 M KCl_2). Nucleosomes were heat shifted at 37° for 1 hour to uniformly position the octamer on the 147 bp DNA template. The nucleosomes were purified from excess DNA and unbound protein using a Prep Cell Model 491 purification system (Bio-Rad) and analyzed by native – PAGE [21].

Nucleosomal arrays were reconstituted onto 208-12-5S rDNA as described [24]. Briefly, equimolar ratios of histone octamers containing H2A, H2B, H4 and H3 or H3K56Q were mixed with the 208-12 DNA template in TE buffer (10 mM Tris-HCl, 0.25 mM EDTA, pH 7.8) containing 2.0 M $NaCl_2$, followed by step-wise salt gradient dialysis to low salt TEN buffer (2.5 mM $NaCl_2$-TE) [24,25].

Nucleosome crystallization

Nucleosomes containing H3K56Q and H3K56E were crystallized by using salting in vapor diffusion at nucleosome concentrations ranging from 8–10 mg/ml and solution conditions of 36 mM KCl, 40 mM $MnCl_2$, 5 mM K-cacodylate and 36 mM KCl, 42 mM $MnCl_2$, 5 mM K-cacodylate. The crystals were soaked in 24% 2-methyl, 2,4-pentanediol (MPD), 5% trehalose, 40.0 mM KCl, 37.0 mM $MnCl_2$ 5.0 mM K-Cacodylate, pH 6.0 [1]. X-ray data was collected at the Advanced Light Source (beam line 4.2.2). The data was processed with Denzo and Scalepack. PDB entry 1KX5 was used as a search model for molecular replacement. Molecular replacement and further refinement was done with CNS [26]. Coot was used for model building [27].

Analytical ultracentrifugation

Sedimentation velocity studies were carried out using a Beckman XL-A analytical ultracentrifuge using absorbance optics. Samples were mixed to a final A_{260} of 0.6 – 0.8 and equilibrated at 20° C. for one hour prior to sedimentation. Nucleosomal arrays were sedimented at 18–25,000 rpm with radial increments of 0.001cm. V-bar and ρ were calculated using Ultrascan v9.4 for windows.

Folding and oligomerization of nucleosomal arrays

To assay folding, nucleosomal arrays were diluted with TEN buffer to a final concentration of 2.0 mM $MgCl_2$ and a final A_{260} of 0.6–0.8 and subjected to sedimentation velocity. Boundaries was analyzed using the improved method of van Holde and Weischet [28] to obtain the integral distribution of sedimentation coefficients, G(s), using UltraScan v9.4 for windows. The average sedimentation coefficient (s_{mid}) was defined as the sedimentation coefficient at the boundary midpoint (boundary fraction = 0.5).

To assay oligomerization, differential centrifugation was used as previously described [29, 30]. Briefly, nucleosome arrays were diluted to an A_{260} = 1.2 with TEN buffer. Arrays were mixed with $MgCl_2$-TEN buffer, incubated for five minutes at room temperature and then centrifuged in a bench-top microfuge at 13,000 RPM (~16,000 × g) for 5 min. The A_{260} of the supernatant was then determined in a Beckman DU 800 Spectrophotometer. Data were expressed as a percentage of the total sample that remained in the supernatant as a function of $MgCl_2$. The Mg^{50} is defined as the $MgCl_2$ concentration at which the sample was 50% oligomerized [29,30].

Results

The crystal structures of nucleosomes containing H3K56Q and H3K56E

We used site directed mutagenesis of H3 to mimic acetylation (H3K56Q), and to introduce a more extreme disturbance at this site by changing the charge from positive to negative (H3K56E). Recombinant H3 containing H356Q or H3K56E were assembled into histone octamers together with recombinant H2A, H2B, and H4. Mono-nucleosomes were reconstituted onto palindromic α-sat DNA [1]. Both mutant nucleosomes were indistinguishable from wild type unmodified nucleosomes based on heat-shifted mobility changes in EMSA assays (Figure 1A, B).

We determined the crystal structure of nucleosomes reconstituted with H3K56Q and H3K56E to a resolution of 3.8 and 3.2 Å respectively, using molecular replacement. Table 1 summarizes data collection and refinement statistics for both datasets. H3K56 is located near the entry and exit point of nucleosomal DNA (Fig. 2A, B). The N epsilon group of H3K56 has a distance of ~ 4 Å to the nearest phosphate group in nucleosomal DNA (Fig. 2C). The mutation of H3K56 to Q or E had no effect on the overall structure of the nucleosome, as revealed by rmsds of < 0.5 when comparing either structure to the wild type nucleosome. The H356E side chain is clearly visible in the electron density generated in omit maps (Fig. 2C). The acidic side chain rotates away from the DNA and towards the solvent. The density for H3-56Q is not visible due to the relatively low resolution of this structure. However, the main conformation of the main chain of the histone and the C β atom of H356Q is not altered compared to the wild type structures.

Importantly, DNA conformation was also unchanged in both particles compared to wild type nucleosomes. This was not unexpected, since the distance between H3K56 and the DNA phosphodiester backbone is too long for a hydrogen bond, and since there is plenty of space for the mutated amino acid to avoid charge-charge interference. Because the side chain is free to rotate, it is unlikely to cause charge-charge repulsion with the DNA. It has been previously observed that the acetylation of H3K56 results in increased breathing of DNA ends [20]. Crystal packing stabilizes the DNA in a ‘closed’ conformation [31], and thus our results are entirely consistent with this observation.

H3K56Q affects oligomerization of nucleosomal arrays that are depleted of nucleosomes

In vitro chromatin condensation consists of two reversible salt-dependent structural transitions: folding (mediated by short-range nucleosome – nucleosome interactions within one nucleosomal array) and oligomerization (mediated by inter-array interactions) [2,8,9]. To investigate the effect of H3K56 modification on higher order chromatin structure, we assembled model nucleosomal arrays from 208-12 DNA and histone octamers containing the acetylation mimic, H3K56Q. The condensation behavior of wild type and mutant nucleosomal arrays via inter-array interactions was then determined as a function of $MgCl_2$ concentration. Because the acetylation of H3K56 is predominantly associated with chromatin assembly and nucleosome-free genomic regions, we wanted to test the effect of H3K56Q on the condensation properties of not only saturated templates, but subsaturated templates containing nucleosome-free repeats [25].

The oligomerization curves for nucleosomal arrays that had an average ~11 bound histone octamers per 208-12 DNA template are shown in Fig. 3A, black symbols. The degree of saturation was determined by sedimentation velocity in TEN buffer ($s_{midpoint}$ = 25–26.5 S; data not shown) as described [24,25]. Under these conditions, the $MgCl_2$ concentration at which the sample was 50% oligomerized (Mg^{50}) of H3K56Q arrays was indistinguishable from wild type arrays. However, when the oligomerization experiment was repeated with

subsaturated nucleosomal arrays containing an average of only ~8 histone octamers/template ($s_{midpoint}$ = 21–22 S; data not shown), the oligomerization curve and Mg^{50} of the H3K56Q arrays were right-shifted relative to wild type (Fig. 3A, open symbols). A summary of the oligomerization data obtained over a wide range of saturation levels is shown in Fig. 3B. Data are plotted as Mg^{50} against the number of nucleosomes as determined by sedimentation coefficient in TEN. The data points are fit with a linear regression to demonstrate the overall trend, even though the distribution of points for H3K56Q is suggestive of nonlinear behavior. The results showed two clear trends. First, the Mg^{50} of the wild type arrays increased linearly as the extent of saturation decreased, consistent with previous results [32]. Second H3K56Q had a major effect on oligomerization of highly to moderately subsaturated arrays. Of note, the effect of K56Q on oligomerization was greater than the effect of the loss of histone octamers per se. These data demonstrate that the H3K56Q mutation is able to significantly disrupt cooperative, inter-array interactions when the arrays contain nucleosome-free regions.

Folding of nucleosomal arrays is unaffected by the H3K56Q mutation

We next examined the salt-dependent folding of wild type and H3K56Q nucleosomal arrays as a function of array saturation. Folding is assayed increases in the sedimentation coefficient at lower salt concentrations than cause oligomerization. S-values were identical for wild type and H3K56Q arrays in low salt TEN at all levels of saturation. Samples were exposed to 1.75 mM $MgCl_2$ to induce folding and subjected to sedimentation velocity in the analytical ultracentrifuge. Data were analyzed to obtain the integral distribution of sedimentation coefficients across the boundaries [28]. Figure 4A shows the data obtained for saturated arrays. Both the wild type and H3K56Q arrays folded robustly as indicated by the right-shifted sedimentation coefficient distributions that ranged as high as 55S [2]. Importantly, the wild type and H3K56Q profiles were essentially identical, indicating no effect of this modification on folding under these conditions. A graph of $s_{midpoint}$ against the number of nucleosomes per template confirms that wild type and K56Q arrays fold identically over a wide range of nucleosome saturated levels (Fig. 4B). These data suggest that H3K56Q does not affect folding of nucleosomal arrays.

Discussion

Posttranslational modifications of histones have the potential to alter chromatin structure at many levels. Modification or amino acid substitutions of the histone tails (e.g. [8,9,33] or introduction of histone variants to alter the nucleosome surface (e.g. [34,35]) can change higher order chromatin folding and oligomerization. Post-translational modifications of histones can also have moderate effects on accessibility and DNA conformation in a mono-nucleosome [36–39], and may alter the ability of histones to engage in histone-histone and histone-DNA interactions, with potential effects on nucleosome stability as was recently observed for the acetylation of H3K56 [20]. It is therefore important to characterize the effect of each histone post-translational modification at multiple structural levels and in different contexts.

The vast majority of histone modifications are located in the flexible histone tails, with little if any potential to impact the structure of the nucleosome per se. However, an increasing number of posttranslational modifications are being identified in the structured region of the histones, with several on side chains near the DNA. Thus far three from the latter category have been characterized biophysically and structurally. The dimethylation of H3K79 has no effect on either the structure nucleosomes or the condensation of nucleosomal arrays [8]; the acetylation of H3K115 and H3K122 increases the rate of thermal repositioning [40], with no implications for the structure (M.L. Dechassa and K.L., unpublished); and the acetylation of H3K56 results in subtle changes in the exposure rate of DNA ends in mononucleosomes [20].

H3K56Q mimics constitutive acetylation in that it causes reduced superhelicity of plasmid chromatin isolated from yeast cells and more rapid nuclease digestion of cellular chromatin [16,41] and thus represents a good model for structural studies of H3K56Ac. We find that the substitution of H3K56 with either Q or E (resulting in an acetylation mimic or charge reversal, respectively), results in no discernable structural changes either in the histone octamer or in the path of the DNA. Since the canonical crystal packing of nucleosome entails base stacking of the DNA as it enters and exits the nucleosome [31], the crystal lattice selects for nucleosomes in which the DNA is in close contact with the histone octamer; and thus subtle differences in DNA dynamics, as demonstrated by Neumann and colleagues [20] cannot be detected through x-ray crystallography.

Lysine 56 acetylation is an abundant modification of newly synthesized histone H3 molecules that are incorporated during S phase and during DNA damage repair [42]. Our finding that the acetylation-mimic H3K56Q affects the oligomerization of nucleosomal arrays *only* in the context of subsaturated arrays containing nucleosome-free regions is consistent with this important role. The oligomerization of nucleosomal arrays reflects long-range interactions between nucleosomes that are distinct from the short-range interactions responsible for array folding [2]. The independence of the two condensation transitions is reinforced by our result that the same K56Q mutation that disrupts oligomerization of subsaturated nucleosomal arrays has no effect on array folding, irrespective of their saturation level.

At this point one can only speculate on the physical basis for the effect observed with subsaturated arrays. It seems likely that our results are related to the increased site exposure of nucleosomal DNA observed by Neumann and colleagues in H3K56Ac nucleosomal arrays [19]. We speculate that site exposure may be more pronounced in arrays with multiple long nucleosome free regions, which serves to free up more linker DNA in the subsaturated arrays. This subsequently would require more $MgCl_2$ to induce oligomerization, as we have observed. It is also possible that H3K56 constitutes a surface area of the nucleosome that interacts with the histone tails during oligomerization, but not folding, and that H3K56Ac is more effective at disrupting such an interaction if there are large gaps in the array. Clearly, further experiments are required to dissect the molecular basis for the unique behavior of subsaturated arrays during oligomerization.

Our findings have several important ramifications for genomic regions harboring nucleosomes with acetylated H3K56. The presence of genomic chromatin containing nucleosome free regions is linked to processes involving increased DNA accessibility, such as transcription, repair, and replication [11–14,16,17]. As discussed above, H3K56Ac tends to be associated with the nucleosomes in and around nucleosome free regions. The surprising observation that oligomerization of nucleosomal arrays containing nucleosome free regions is selectively affected by the K56Q mutation, with H3K56Q destabilizing inter-array interactions in vitro, strongly suggests that H3K56 acetylation is one of the mechanisms employed to keep chromatin with nucleosome free regions accessible at the higher order level. Both our data with H3K56Q, and those obtained previously with H3K56Ac [20], indicate that this modification does not function at the level of local chromatin fiber folding. However, we note that folding is intrinsically inhibited by nucleosome free regions [22,23]. Furthermore, the destabilization of $(H3\text{-}H4)_2$ tetramer-DNA interactions by H3K56Ac (A. J. Andrews and K.L., unpublished) may also facilitate nucleosome eviction events at RNAPII promoters, subsequent to the removal of the H2A-H2B dimer by ATP-dependent nucleosome remodeling enzymes or histone chaperones [43,44]. Regardless of the mechanism(s) involved, identification of a modification that specifically targets chromatin with nucleosome free regions is novel. Our data are consistent with a model in which the tertiary interactions of subsaturated nucleosomal arrays are regulated by acetylation of H3 K56, and disruption of such interactions by H3 K56Ac

has a significant impact on DNA repair, transcription, and the stability of stalled replication forks.

Acknowledgments

We thank Teri McLain from the W. M. Keck PEPF for histones, Pamela N. Dyer and Alyson White for DNA preparations, Mark van der Woerd and Jay Nix for help with structure determination. Supported by the NIH (GM045916 to JCH, GM54096 to CLP, and GM061909 to KL.) Coordinate files for the two structures have been deposited at the protein data bank (PDB ID 3KWQ and 3KXB).

References

1. Luger K, Maeder AW, Richmond RK, Sargent DF, Richmond TJ. Crystal structure of the nucleosome core particle at 2.8 Å resolution. Nature 1997;389:251–259. [PubMed: 9305837]
2. Hansen JC. CONFORMATIONAL DYNAMICS OF THE CHROMATIN FIBER IN SOLUTION: Determinants, Mechanisms, and Functions. Annu Rev Biophys Biomol Struct 2002;31:361–392. [PubMed: 11988475]
3. Kouzarides T. Chromatin modifications and their function. Cell 2007;128:693–705. [PubMed: 17320507]
4. Jenuwein T, Allis CD. Translating the histone code. Science 2001;293:1074–1080. [PubMed: 11498575]
5. Andrews AJ, Luger K. Histone Modifications: Chemistry and Structural Consequences. Wiley Encyclopedia of Chemical Biology 2009;1:275–284.
6. Marmorstein R, Trievel RC. Histone modifying enzymes: structures, mechanisms, and specificities. Biochim Biophys Acta 2009;1789:58–68. [PubMed: 18722564]
7. Taverna SD, Li H, Ruthenburg AJ, Allis CD, Patel DJ. How chromatin-binding modules interpret histone modifications: lessons from professional pocket pickers. Nature Structural & Molecular Biology 2007;14:1025–1040.
8. Lu X, Simon MD, Chodaparambil JV, Hansen JC, Shokat KM, Luger K. The effect of H3K79 dimethylation and H4K20 trimethylation on nucleosome and chromatin structure. Nature Structural & Molecular Biology 2008;15:1122–1124.
9. Shogren-Knaak M, Ishii H, Sun JM, Pazin MJ, Davie JR, Peterson CL. Histone H4-K16 acetylation controls chromatin structure and protein interactions. Science 2006;311:844–847. [PubMed: 16469925]
10. Robinson PJ, An W, Routh A, Martino F, Chapman L, Roeder RG, Rhodes D. 30 nm chromatin fibre decompaction requires both H4-K16 acetylation and linker histone eviction. J Mol Biol 2008;381:816–825. [PubMed: 18653199]
11. Xu F, Zhang K, Grunstein M. Acetylation in histone H3 globular domain regulates gene expression in yeast. Cell 2005;121:375–385. [PubMed: 15882620]
12. Williams SK, Truong D, Tyler JK. Acetylation in the globular core of histone H3 on lysine-56 promotes chromatin disassembly during transcriptional activation. PNAS 2008;105:9000–9005. [PubMed: 18577595]
13. Chen CC, Carson JJ, Feser J, Tamburini B, Zabaronick S, Linger J, Tyler JK. Acetylated lysine 56 on histone H3 drives chromatin assembly after repair and signals for the completion of repair. Cell 2008;134:231–243. [PubMed: 18662539]
14. Tjeertes JV, Miller KM, Jackson SP. Screen for DNA-damage-responsive histone modifications identifies H3K9Ac and H3K56Ac in human cells. EMBO J 2009;28:1878–1889. [PubMed: 19407812]
15. Kaplan T, Liu CL, Erkmann JA, Holik J, Grunstein M, Kaufman PD, Friedman N, Rando OJ. Cell cycle- and chaperone-mediated regulation of H3K56ac incorporation in yeast. PLoS Genet 2008;4:e1000270. [PubMed: 19023413]
16. Masumoto H, Hawke D, Kobayashi R, Verreault A. A role for cell-cycle-regulated histone H3 lysine 56 acetylation in the DNA damage response. Nature 2005;436:294–298. [PubMed: 16015338]

17. Das C, Lucia MS, Hansen KC, Tyler JK. CBP/p300-mediated acetylation of histone H3 on lysine 56. Nature. 2009

18. Ferreira H, Somers J, Webster R, Flaus A, Owen-Hughes T. Histone tails and the H3 alphaN helix regulate nucleosome mobility and stability. Mol Cell Biol 2007;27:4037–4048. [PubMed: 17387148]

19. Neumann H, Peak-Chew SY, Chin JW. Genetically encoding N(epsilon)-acetyllysine in recombinant proteins. Nat Chem Biol 2008;4:232–234. [PubMed: 18278036]

20. Neumann H, Hancock SM, Buning R, Routh A, Chapman L, Somers J, Owen-Hughes T, van Noort J, Rhodes D, Chin JW. A method for genetically installing site-specific acetylation in recombinant histones defines the effects of h3 k56 acetylation. Mol Cell 2009;36:153–163. [PubMed: 19818718]

21. Dyer PN, Edayathumangalam RS, White CL, Bao Y, Chakravarthy S, Muthurajan UM, Luger K. Reconstitution of nucleosome core particles from recombinant histones and DNA. Methods Enzymol 2004;375:23–44. [PubMed: 14870657]

22. Schwarz PM, Hansen JC. Formation and stability of higher order chromatin structures. Contributions of the histone octamer. J Biol Chem 1994;269:16284–16289. [PubMed: 8206934]

23. Georgel P, Demeler B, Terpening C, Paule MR, van Holde KE. Binding of the RNA polymerase I transcription complex to its promoter can modify positioning of downstream nucleosomes assembled in vitro. J Biol Chem 1993;268:1947–1954. [PubMed: 8420969]

24. Hansen JC, van Holde KE, Lohr D. The mechanism of nucleosome assembly onto oligomers of the sea urchin 5 S DNA positioning sequence. J Biol Chem 1991;266:4276–4282. [PubMed: 1900288]

25. Hansen JC, Lohr D. Assembly and structural properties of subsaturated chromatin arrays. J Biol Chem 1993;268:5840–5848. [PubMed: 8449950]

26. Brunger AT. Version 1.2 of the Crystallography and NMR system. Nat Protoc 2007;2:2728–2733. [PubMed: 18007608]

27. Emsley P, Cowtan K. Coot: model-building tools for molecular graphics. Acta Crystallogr D Biol Crystallogr 2004;60:2126–2132. [PubMed: 15572765]

28. Demeler B, van Holde KE. Sedimentation velocity analysis of highly heterogeneous systems. Anal Biochem 2004;335:279–288. [PubMed: 15556567]

29. Lu X, Klonoski JM, Resch MG, Hansen JC. In vitro chromatin self-association and its relevance to genome architecture. Biochem Cell Biol 2006;84:411–417. [PubMed: 16936814]

30. Gordon F, Luger K, Hansen JC. The core histone N-terminal tail domains function independently and additively during salt-dependent oligomerization of nucleosomal arrays. J Biol Chem 2005;280:33701–33706. [PubMed: 16033758]

31. Suto RK, Edayathumangalam RS, White CL, Melander C, Gottesfeld JM, Dervan PB, Luger K. Crystal Structures of Nucleosome Core Particles in Complex with Minor Groove DNA-binding Ligands. J Mol Biol 2003;326:371–380. [PubMed: 12559907]

32. Schwarz PM, Felthauser A, Fletcher TM, Hansen JC. Reversible oligonucleosome self-association: dependence on divalent cations and core histone tail domains. Biochemistry 1996;35:4009–4015. [PubMed: 8672434]

33. Horn PJ, Crowley KA, Carruthers LM, Hansen JC, Peterson CL. The SIN domain of the histone octamer is essential for intramolecular folding of nucleosomal arrays. Nat Struct Biol 2002;9:167–171. [PubMed: 11836537]

34. Abbott DW, Ivanova VS, Wang X, Bonner WM, Ausio J. Characterization of the stability and folding of H2A.Z chromatin particles: implications for transcriptional activation. J Biol Chem 2001;276:41945–41949. [PubMed: 11551971]

35. Fan JY, Gordon F, Luger K, Hansen JC, Tremethick DJ. The essential histone variant H2A.Z regulates the equilibrium between different chromatin conformational states.[see comment][erratum appears in Nat Struct Biol 2002 Apr;9(4):316]. Nature Structural Biology 2002;9:172–176.

36. Lee DY, Hayes JJ, Pruss D, Wolffe AP. A positive role for histone acetylation in transcription factor access to nucleosomal DNA. Cell 1993;72:73–84. [PubMed: 8422685]

37. Bauer WR, Hayes JJ, White JH, Wolffe AP. Nucleosome structural changes due to acetylation. J Mol Biol 1994;236:685–690. [PubMed: 8114086]

38. Polach KJ, Lowary PT, Widom J. Effects of core histone tail domains on the equilibrium constants for dynamic DNA site accessibility in nucleosomes. J Mol Biol 2000;298:211–223. [PubMed: 10764592]

39. Widlund HR, Vitolo JM, Thiriet C, Hayes JJ. DNA sequence-dependent contributions of core histone tails to nucleosome stability: differential effects of acetylation and proteolytic tail removal. Biochemistry 2000;39:3835–3841. [PubMed: 10736184]

40. Manohar M, Mooney AM, North JA, Nakkula RJ, Picking JW, Edon A, Fishel R, Poirier MG, Ottesen JJ. Acetylation of histone H3 at the nucleosome dyad alters DNA-histone binding. J Biol Chem 2009;284:23312–23321. [PubMed: 19520870]

41. Recht J, Tsubota T, Tanny JC, Diaz RL, Berger JM, Zhang X, Garcia BA, Shabanowitz J, Burlingame AL, Hunt DF, Kaufman PD, Allis CD. Histone chaperone Asf1 is required for histone H3 lysine 56 acetylation, a modification associated with S phase in mitosis and meiosis. PNAS 2006;103:6988–6993. [PubMed: 16627621]

42. Tsubota T, Berndsen CE, Erkmann JA, Smith CL, Yang L, Freitas MA, Denu JM, Kaufman PD. Histone H3-K56 acetylation is catalyzed by histone chaperone-dependent complexes. Mol Cell 2007;25:703–712. [PubMed: 17320445]

43. Bruno M, Flaus A, Stockdale C, Rencurel C, Ferreira H, Owen-Hughes T. Histone H2A/H2B dimer exchange by ATP-dependent chromatin remodeling activities. Mol Cell 2003;12:1599–1606. [PubMed: 14690611]

44. Vicent GP, Nacht AS, Smith CL, Peterson CL, Dimitrov S, Beato M. DNA instructed displacement of histones H2A and H2B at an inducible promoter. Mol Cell 2004;16:439–452. [PubMed: 15525516]

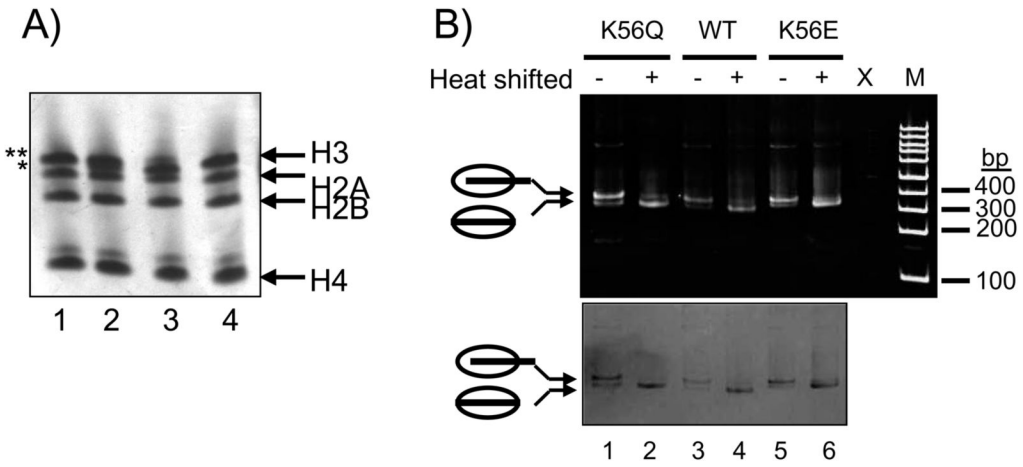

Figure 1. Nucleosomes reconstituted with H3K56Q and K56E

A) Mutation of H3K56 to Q or E results in reduced electrophoretic mobility on triton-urea gels. 4 μg of refolded histone octamers containing mutations to histone H3K56Q (lane 1), H3K56Q with WT H3 (lane 2), WT (lane 3) and H3K56E (lane 4) were loaded and electrophoresed on an AU-PAGE gel stained with coomassie blue. (*) indicates wild type H3 and (**) indicates H3K56Q and H3K56E mobility. **B)** Reconstituted nucleosomes containing H3-K56 mutations have a similar ability to heat shift. Nucleosomes containing H3 K56Q (lanes 1 and 2), WT H3 (lane 3 and 4) and H3 K56E (lane 5 and 6) reconstituted with 147 bp α-Sat DNA. Nucleosomes were heat shifted (+) for 1 hour at 37°C (lanes 2, 4 and 6). Samples were separated on a 5 % native polyacrylamide gel and stained with ethidium bromide (top) and Imperial Protein Stain (Pierce) (bottom). M indicates 100 bp marker.

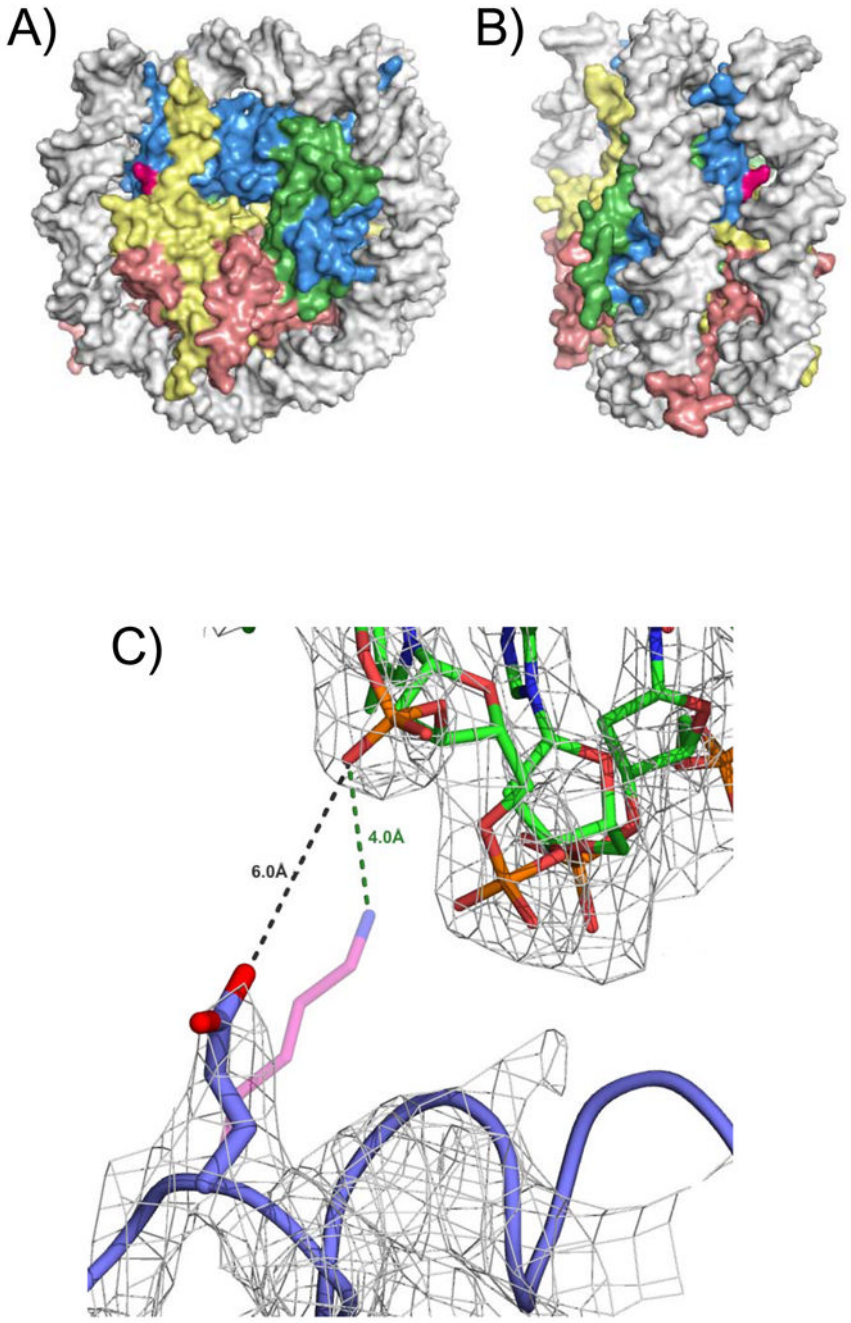

Figure 2. Structural analysis of nucleosomes reconstituted with H3K56E

A) Location of H3K56 in the nucleosome. H3 is shown in blue, H4 in green, H2A in yellow, and H2B in red. H3K56 is indicated in magenta. The nucleosome is viewed down the superhelical axis. **B)** as A), but rotated around the y-axis by about 75 degrees. **C)** Detailed view of the structure of a nucleosome with H3K56E, superimposed onto the wild type structure. Distances between the side chains and DNA are indicated. Electron density (2Fo-Fc) is contoured at 1 sigma.

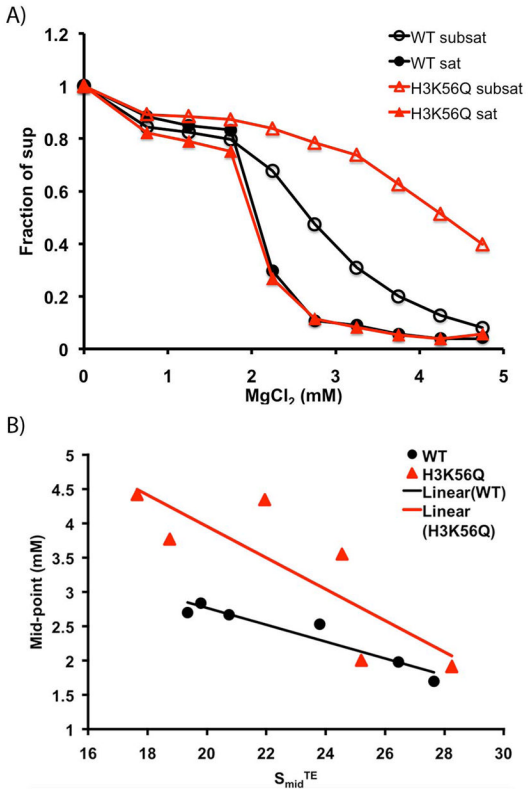

Figure 3. H3K56Q disrupts intermolecular oligomerization of subsaturated nucleosomal arrays

A) Intermolecular oligomerization assay. Nucleosomal arrays were incubated with varying concentrations of $MgCl_2$, followed by centrifugation. The fraction of array remaining in the supernatant is plotted as a function of $MgCl_2$ concentration. Samples of the following saturation levels, indicated by S_{mid}^{TE} were analyzed: black circles, filled: wild type, 26.5S; black circles, open: wild type 20.8S; red triangles, filled: H3K56, 25.2S; red triangles, open: H3K56Q, 22S. **B)** Effect of nucleosomal array saturation on intermolecular oligomerization. Nucleosomal arrays were reconstituted at various ratios of histone octamer to 208 bp 5S DNA repeats. Arrays were analyzed by sedimentation velocity analysis in TE buffer to determine their degree of saturation (S_{mid}^{TE}). $MgCl_2$ concentration required for half of the arrays to remain in the supernatant is plotted as a function of S_{mid}^{TE}. Black circles, wild type; red triangles, H3K56Q. Lines represent a linear regression through the data points.

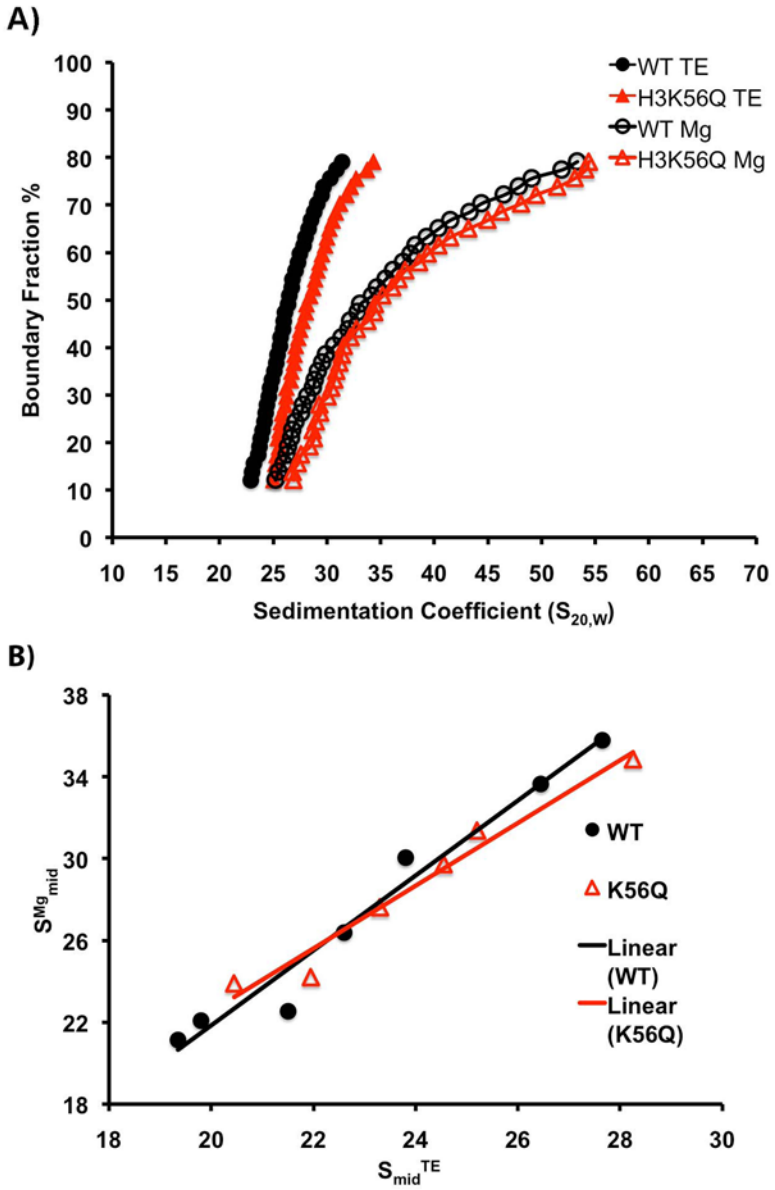

Figure 4. H3K56Q does not affect intramolecular folding of nucleosomal arrays

A) Sedimentation velocity analysis of 208-12 nucleosomal arrays in TE (10mM Tris-HCl (pH7.4) and 0.25mM EDTA) or TE with 1.75mM $MgCl_2$. Integrated sedimentation coefficient distributions of nucleosomal arrays were determined by sedimention velocity and van Holde-Weischet analysis. $S_{20,w}$ is the sedimentation coefficient corrected to water at 20 °C. Black circles: wild type arrays in TE; open circles: wild type arrays in $MgCl_2$. Red triangles: H3K56Q arrays in TE; open triangles, H3K56Q arrays in $MgCl_2$. **B)** Intramolecular folding of nucleosomal arrays at varying levels of nucleosome occupancy. Black circles: wild type arrays, red triangles: H3K56Q arrays. Nucleosomal arrays were reconstituted at various ratios of histone octamer to 208 bp 5S DNA repeats. Arrays were analyzed by a sedimentation velocity analysis in either TE or TE + 1.75 mM $MgCl_2$ buffers. The S_{mid}^{TE} and S^{Mg}_{mid} are defined as the sedimentation coefficients at the boundary fraction = 0.5 in TE and TE with 1.75mM $MgCl_2$, respectively. Lines represent a linear regression through the data points.

Table 1

Data collection and refinement statistics for nucleosomes reconstituted with H3K56Q and H3K56E.

Data Collection	**K56Q**	**K56E**
Space Group	$P2_12_12_1$	$P2_12_12_1$
Cell dimensions		
a, *b*, *c* (Å)	109.54, 105.56, 180.65	109.51, 105.67, 180.56
α,β,γ	90, 90, 90	90, 90, 90
Resolution (Å)	20 (3.78)	20 (3.2)
R_{sym} or R_{merge}	0.109 (0.358)	0.055 (0.342)
I/σ*I*	6.0 (4.3)	19.53 (3.9)
Completeness %	100 (100)	81(73.6)
Redundancy	7.23 (7.41)	2.2(2.0)
Refinement		
Resolution (Å)	3.78	3.2
Observations	308,860 (26,559)	372,562 (35,641)
R_{work}/R_{free}	0.2684/0.3146	0.2845/0.2926
No. Atoms		
Protein	6012	5831
DNA	5980	5980
B-factors		
Protein	87.5	50.1
DNA	147	109.6
R.m.s. deviations		
Protein bond lengths	0.013	0.013
DNA bond lengths	0.005	0.005
Protein bond angle	1.711	1.642
DNA bond angle	0.808	.762